

Tema: Estruturas de aço e mistas de aço e concreto

## ELASTOPLASTIC ANALYSIS WITH NONLINEAR HARDENING LAW FOR STEEL STRUCTURES WITH COMPACT CROSS-SECTIONS\*

Yuri Teixeira<sup>1</sup>  
Eduardo M. B. Campello<sup>2</sup>

### Abstract

In this work, we present the formulation and numerical implementation of a simple elastoplastic constitutive equation for geometrically exact rod models with consideration of cross-sectional warping. Given the kinematical hypothesis of non-deformability of the cross-section in the projection of its plane, we work with compact cross-sections and assume that the plastic deformations occur due only to the cross-sectional normal stresses, thereby allowing us to work under a simple uniaxial framework. Our approach adopts a standard additive decomposition of the strains together with a linear elastic relation for the elastic part of the deformations. Both ideal plasticity and plasticity with (nonlinear) isotropic hardening are considered. The resulting equation is implemented within a finite element rod model and is validated by means of several numerical examples. The rod model considers warping effects and has 7 degrees of freedom. We believe that a simple elastoplastic model embedded within a robust rod finite element is a useful tool for the analysis of thin-walled rod structures, such as, e.g., steel structures.

**Keywords:** Plasticity; Elastoplastic constitutive equation; Rod model; Finite elements; Steel structures

## ANÁLISE NÃO-LINEAR ELASTOPLÁSTICA DE ESTRUTURAS DE AÇO COM PERFIS DE SEÇÃO TRANSVERSAL COMPACTA\*

### Resumo

Neste trabalho, apresentamos a formulação e implementação computacional de uma equação constitutiva elastoplástica simples para modelos de barra geometricamente exatos com consideração do empenamento. Dada a hipótese cinemática de não deformabilidade da seção transversal da barra na projeção de seu plano, trabalhamos com seções transversais compactas e assumimos que as deformações plásticas ocorrem devido apenas às tensões normais à seção transversal, permitindo-nos trabalhar com um modelo constitutivo uniaxial simples. Nossa abordagem adota uma decomposição aditiva das deformações, com uma relação linear para a parte elástica. Tanto plasticidade ideal quanto plasticidade com encruamento isotrópico (não-linear) são considerados. A equação resultante é implementada em um modelo de elementos finitos de barras e é validada em diversos exemplos numéricos. O modelo de barra considera efeitos de empenamento da seção transversal e possui 7 graus de liberdade. O resultado é um modelo elastoplástico simples combinado com um elemento finito de barra robusto que se mostra útil para a análise de estruturas reticuladas constituídas por barras de seção transversal de paredes delgadas, mas que não estão suscetíveis a instabilidades localizadas, como, por exemplo, estruturas constituídas de perfis de aço laminados e soldados de seção compacta.

**Palavras-chave:** Plasticidade; Equação constitutiva elastoplástica; Modelo de barra; Elementos finitos; Estruturas de aço

<sup>1</sup> Arquiteto e Urbanista, Estudante de Mestrado do Programa de Pós-graduação em Engenharia Civil, Escola Politécnica da USP, São Paulo, São Paulo, Brasil.

<sup>2</sup> Engenheiro Civil, Professor Doutor do Departamento de Engenharia de Estruturas e Geotécnica da USP e pesquisador (nível 2) do CNPq, São Paulo, São Paulo, Brasil.

\* Contribuição tecnológica ao **Construmetal 2016** – Congresso Latino-americano da Construção Metálica – 20 a 22 de setembro de 2016, São Paulo, SP, Brasil.

## 1. INTRODUCTION

One of the motivations for the development of scientific research in engineering is the optimization of structural elements with respect to the relation between quantity of material and capacity to perform its function. This greater efficiency is acquired through application of ever more accurate analyses of physical behavior of the structural element in the designed structure. This minimizes the excess of material used to attain the necessary performance and safety. For steel structural elements, one of the biggest barriers to the advance in this area is the complexity of methods of analysis with consideration of geometrical nonlinearity (GNL) and the description of the boundaries of elastic and plastic deformation regimens of the material, i.e. consideration of material nonlinearity (MNL). Given the characteristics of structural steel material and the slender geometry of these elements, effects of GNL and MNL are relevant for many design criteria, most notably in statically indeterminate plane and spatial frames.

The design of structural elements to work in plastic regimen considers resistances greater than those in elastic regimen and allow a gain of efficiency maintaining the necessary safety in design with adequate loading and geometric conditions. This consideration involves the analysis of the structure with partial plastification of the cross-sections as well as, in statically indeterminate structures, the formation of full plastic hinges.

The classical methods of structural analysis with consideration of plasticity and GNL are laborious and have been giving way to analyses with mathematical models that allow a better use of the processing capacity of current computers. The development and implementation of constitutive models with consistent kinematical formulations is, because of that, a subject that has attracted researchers over many recent years.

In this work, we present the formulation and implementation of a simple elastoplastic constitutive equation for geometrically exact thin-walled rod models. We assume that the plastic deformations may occur due only to the cross-sectional normal stresses, thereby allowing us to work under a simple uniaxial framework. Our approach adopts a standard additive decomposition of the strains together with a linear elastic relation for the elastic part of the deformation. Both ideal plasticity and plasticity with (linear) isotropic hardening are considered. The model is implemented within a finite element thin-walled rod model and is validated by means of numerical examples. We believe that simple elastoplastic models combined with robust thin-walled rod finite elements may be a useful tool for the analysis of thin-walled rod structures, such as, e.g., steel structures.

Throughout this text, italic Greek or Latin lowercase letters ( $a, b, \dots, \alpha, \beta, \dots$ ) denote scalar quantities, bold italic Greek or Latin lowercase letters ( $\mathbf{a}, \mathbf{b}, \dots, \boldsymbol{\alpha}, \boldsymbol{\beta}, \dots$ ) denote vectors and bold italic Greek or Latin capital letters ( $\mathbf{A}, \mathbf{B}, \dots$ ) denote second-order tensors in a three-dimensional Euclidean space. Summation convention over repeated indices is adopted, with Greek indices ranging from 1 to 2 and Latin indices from 1 to 3.

## 2. GEOMETRICALLY EXACT ROD KINEMATICS

The kinematical rod model that is the basis of this work had its first developments in the works of Pimenta and Yoho (1993), with a first implementation in Campello (2000). It is a geometrically exact formulation in which shear deformation due to bending and cross-section warping due to combined bending and non-uniform torsion are explicitly taken into account. A straight reference configuration is assumed for the rod axis at the outset. A local orthonormal system  $\{e_1^r, e_2^r, e_3^r\}$  with corresponding coordinates  $\{x_1, x_2, x_3\}$  is defined in this configuration, with vectors  $e_\alpha^r$  ( $\alpha = 1, 2$ ) placed on the rod's cross-section and  $e_3^r$  placed along the rod axis as shown in Fig. 1. Points in this configuration are described by the vector field

$$\boldsymbol{\xi} = \boldsymbol{\zeta} + \mathbf{a}^r. \quad (1)$$

---

\* Contribuição tecnológica ao **Construmetal 2016** – Congresso Latino-americano da Construção Metálica – 20 a 22 de setembro de 2016, São Paulo, SP, Brasil.

The rod axis is described by  $\zeta = x_3 e_3$ , where  $x_3 \in L = [0, l]$  is the axis coordinate, with  $l$  being the rod's reference length, and the cross-section is described relative to the rod axis by  $\mathbf{a}^r = x_\alpha e_\alpha$ .

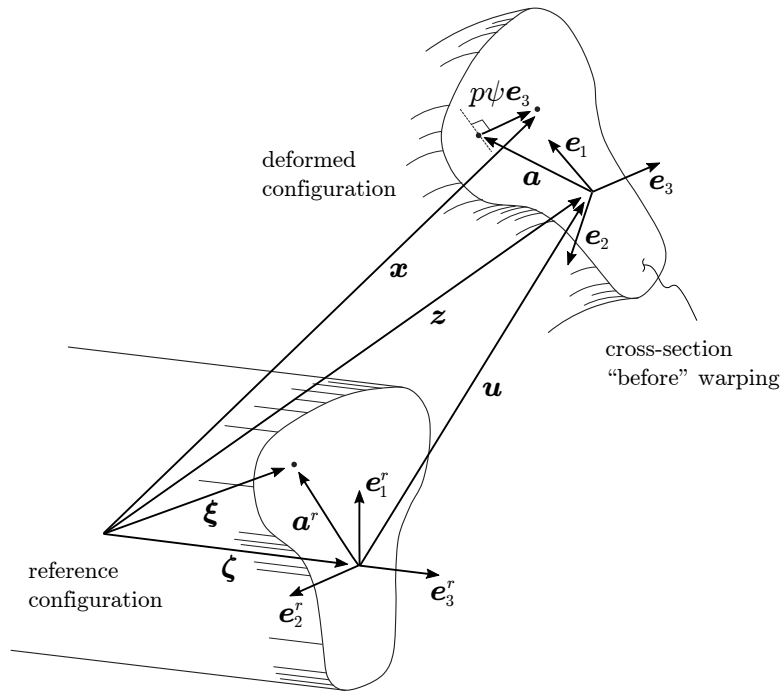


Figure 1: Rod description and kinematics.  
Source: created by the authors.

In the deformed configuration, another orthonormal system  $\{e_1, e_2, e_3\}$  is defined, as depicted in Fig. 1. The deformation of the rod is then described by a vector field  $\mathbf{x}$  such that the position of the material points is expressed by

$$\mathbf{x} = \mathbf{z} + \mathbf{a} + p\psi e_3, \quad (2)$$

where  $\mathbf{z} = \hat{\mathbf{z}}(x_3)$  describes the position of points at the deformed axis,  $\mathbf{a} = \hat{\mathbf{a}}(x_\alpha, x_3)$  defines the position of points at the deformed cross-section *in the projection of its plane*,  $\psi = \hat{\psi}(x_\alpha)$  is a function defining the warping of the cross-section with respect to its shear center (the so-called warping function) and  $p = \hat{p}(x_3)$  is a scalar parameter that gives  $\psi$  its amplitude. Many possibilities exist for the choice of  $\psi$ , as for example the classical Saint-Venant warping function, the Vlasov sectorial area (Vlasov, 1961), or any other function that adequately describes the out-of-plane deformation of the cross-section. In the present work, we adopt a  $\psi$  that is approximated using the finite element method on a bidimensional mesh of the cross-section.

In Eq. (2), and from Fig. 1, one finds that  $\mathbf{z} = \zeta + \mathbf{u}$ , where  $\mathbf{u}$  is the displacement vector of points of the rod axis. Vector  $\mathbf{a}$ , in turn, is obtained by  $\mathbf{a} = \mathbf{Q}\mathbf{a}^r = x_\alpha e_\alpha$ , in which  $\mathbf{Q}$  is the rotation tensor of the cross-section. Accordingly, no cross-sectional in-plane distortion is allowed, but first order shear deformations are accounted for since  $\mathbf{a}$  is not necessarily normal to the deformed axis. Relation  $e_i = \mathbf{Q}e_i^r$  ( $i = 1, 2, 3$ ) holds for the local systems.

The rotation tensor  $\mathbf{Q}$  may be written in terms of the Euler rotation vector  $\boldsymbol{\theta} = \theta e$  by means of the

well-known Euler-Rodrigues formula

$$\mathbf{Q} = \mathbf{I} + \frac{\sin \theta}{\theta} \boldsymbol{\Theta} + \frac{1}{2} \frac{(\sin(\theta/2))^2}{(\theta/2)^2} \boldsymbol{\Theta}^2, \quad (3)$$

in which  $\theta = \|\boldsymbol{\theta}\|$  is the rotation angle of the cross-section and  $\boldsymbol{\Theta} = \text{Skew}(\boldsymbol{\theta})$  is the skew-symmetric tensor whose axial vector is  $\boldsymbol{\theta}$ .

Components of  $\mathbf{u}$  and  $\boldsymbol{\theta}$  on a global Cartesian system along with the scalar parameter  $p$  constitute the seven degrees-of-freedom of this rod model. They are grouped into a vector  $\mathbf{d}$  as follows:

$$\mathbf{d} = \begin{bmatrix} \mathbf{u} \\ \boldsymbol{\theta} \\ p \end{bmatrix}. \quad (4)$$

The deformation gradient  $\mathbf{F}$  is obtained from differentiation of Eq. (2) with respect to  $\boldsymbol{\xi}$ . Using the notation  $(\bullet)' = \partial(\bullet)/\partial x_3$  and  $(\bullet)_{,\alpha} = \partial(\bullet)/\partial x_\alpha$  for derivatives, it is written as

$$\mathbf{F} = \mathbf{Q}(\mathbf{I} + \psi_{,\alpha} p \mathbf{e}_3^r \otimes \mathbf{e}_\alpha^r + \boldsymbol{\gamma}_3^r \otimes \mathbf{e}_3^r), \quad (5)$$

where

$$\boldsymbol{\gamma}_3^r = \boldsymbol{\eta}^r + \boldsymbol{\kappa}^r \times (\mathbf{a}^r + \psi p \mathbf{e}_3^r) + \psi p' \mathbf{e}_3^r, \quad (6)$$

in which

$$\boldsymbol{\eta}^r = \mathbf{Q}^T \mathbf{z}' - \mathbf{e}_3^r \quad \text{and} \quad \boldsymbol{\kappa}^r = \boldsymbol{\Gamma}^T \boldsymbol{\theta}'. \quad (7)$$

With these we can also define the back-rotated deformation gradient

$$\mathbf{F}^r = \mathbf{Q}^T \mathbf{F} = \mathbf{I} + \psi_{,\alpha} p \mathbf{e}_3^r \otimes \mathbf{e}_\alpha^r + \boldsymbol{\gamma}_3^r \otimes \mathbf{e}_3^r, \quad (8)$$

Vector  $\boldsymbol{\gamma}_3^r$  in Eq. (6) can be regarded as the cross-sectional generalized strain vector, with  $\boldsymbol{\eta}^r$  and  $\boldsymbol{\kappa}^r$  of Eq. (7) being the rod's strains (they encompass the axis elongation and the cross-sectional shear and specific rotations). Tensor  $\boldsymbol{\Gamma}$  in Eq. (7)<sub>2</sub> relates the angular velocities vector  $\boldsymbol{\omega}$  to the temporal derivatives of the rotation parameters  $\boldsymbol{\theta}$  and reads as

$$\boldsymbol{\Gamma} = \mathbf{I} + \frac{1}{2} \frac{(\sin(\theta/2))^2}{(\theta/2)^2} \boldsymbol{\Theta} + \frac{1 - (\sin \theta)/\theta}{\theta^2} \boldsymbol{\Theta}^2. \quad (9)$$

Linearization of Eq. (5) with respect to  $\mathbf{d}$  yields the virtual deformation gradient. Using the symbol “ $\delta$ ” to denote linearized or virtual quantities, the result is as follows:

$$\delta \mathbf{F} = \delta \boldsymbol{\Omega} \mathbf{F} + \mathbf{Q}(\psi_{,\alpha} \delta p \mathbf{e}_3^r \otimes \mathbf{e}_\alpha^r + \delta \boldsymbol{\gamma}_3^r \otimes \mathbf{e}_3^r), \quad (10)$$

where  $\delta \boldsymbol{\Omega} = \delta \mathbf{Q} \mathbf{Q}^T$  is a skew-symmetric tensor whose axial vector is denoted by  $\delta \boldsymbol{\omega}$ . One can show that  $\delta \boldsymbol{\omega} = \text{axial}(\delta \mathbf{Q} \mathbf{Q}^T) = \boldsymbol{\Gamma} \delta \boldsymbol{\theta}$ , with  $\boldsymbol{\Gamma}$  given by Eq. (9). The virtual strain vector  $\delta \boldsymbol{\gamma}_3^r$  of Eq. (10) is obtained from linearization of Eq. (6) and reads as

$$\delta \boldsymbol{\gamma}_3^r = \delta \boldsymbol{\eta}^r + \delta \boldsymbol{\kappa}^r \times (\mathbf{a}^r + \psi p \mathbf{e}_3^r) + \psi \delta p' \mathbf{e}_3^r + \psi \delta p \boldsymbol{\kappa}^r \times \mathbf{e}_3^r, \quad (11)$$

in which

$$\delta \boldsymbol{\eta}^r = \mathbf{Q}^T (\delta \mathbf{u}' + \mathbf{Z}' \boldsymbol{\Gamma} \delta \boldsymbol{\theta}) \quad \text{and} \quad \delta \boldsymbol{\kappa}^r = \mathbf{Q}^T (\boldsymbol{\Gamma}' \delta \boldsymbol{\theta} + \boldsymbol{\Gamma} \delta \boldsymbol{\theta}') \quad (12)$$

\* Contribuição tecnológica ao **Construmetal 2016** – Congresso Latino-americano da Construção Metálica – 20 a 22 de setembro de 2016, São Paulo, SP, Brasil.

are obtained from the linearization of Eq. (7). In the above expressions,  $\mathbf{Z}'$  is the skew-symmetric tensor whose axial vector is  $\mathbf{z}'$ , i.e.  $\mathbf{Z}' = \text{Skew}(\mathbf{z}')$ . Let now the first Piola-Kirchhoff stress tensor be expressed in terms of its column-vectors as

$$\mathbf{P} = \boldsymbol{\tau}_i \otimes \mathbf{e}_i^r. \quad (13)$$

Vectors  $\boldsymbol{\tau}_i$  are the nominal stresses acting on a point of the rod according to planes whose normals in the reference configuration are  $\mathbf{e}_i^r$ . One may also write  $\mathbf{P} = \mathbf{Q}\mathbf{P}^r$ , with

$$\mathbf{P}^r = \boldsymbol{\tau}_i^r \otimes \mathbf{e}_i^r \quad (14)$$

as the back-rotated counterpart of  $\mathbf{P}$ . In this case, vectors  $\boldsymbol{\tau}_i^r$  are the back-rotated stress vectors.

The internal virtual work of the rod, with the aid of Eqs. (10) and (13), is given by

$$\delta W_{int} = \int_L \int_A (\mathbf{P} : \delta \mathbf{F}) dA dL \quad (15)$$

where  $A$  is the area of the cross-sections at the reference configuration. Performing integration over the area, we define the following cross-sectional stresses:

$$\begin{aligned} \mathbf{n}^r &= \int_A \boldsymbol{\tau}_3^r dA = V_\alpha \mathbf{e}_\alpha^r + N \mathbf{e}_3^r \\ \mathbf{m}^r &= \int_A (\mathbf{a}^r + \psi p \mathbf{e}_3^r) \times \boldsymbol{\tau}_3^r dA = M_\alpha \mathbf{e}_\alpha^r + T \mathbf{e}_3^r \\ Q &= \int_A ((\boldsymbol{\tau}_\alpha^r \cdot \mathbf{e}_3^r) \psi_{,\alpha} + \boldsymbol{\tau}_3^r \cdot (\boldsymbol{\kappa}^r \times \mathbf{e}_3^r) \psi) dA \\ B &= \int_A (\boldsymbol{\tau}_3^r \cdot \mathbf{e}_3^r) \psi dA. \end{aligned} \quad (16)$$

Components of the first two vectors above are the resultant shear forces ( $V_\alpha$ ), normal force ( $N$ ), bending moments ( $M_\alpha$ ) and torsional moment ( $T$ ) of the cross-sections, whereas  $Q$  and  $B$  are the so-called bi-shear and bi-moment due to the consideration of warping.

Grouping them in a generalized stress vector  $\boldsymbol{\sigma}^r$  and matching them with their corresponding virtual strains in vector  $\delta \boldsymbol{\varepsilon}^r$  we obtain

$$\boldsymbol{\sigma}^r = \begin{bmatrix} \mathbf{n}^r & \mathbf{m}^r & Q & B \end{bmatrix}^T \quad \text{and} \quad \delta \boldsymbol{\varepsilon}^r = \begin{bmatrix} \delta \boldsymbol{\eta}^r & \delta \boldsymbol{\kappa}^r & \delta p & \delta p' \end{bmatrix}^T \quad (17)$$

which are  $8 \times 1$  vectors that can be used to rewrite Eq. (15) as

$$\delta W_{int} = \int_L (\boldsymbol{\sigma}^r \cdot \delta \boldsymbol{\varepsilon}^r) dL. \quad (18)$$

Vector  $\delta \boldsymbol{\varepsilon}^r$  of Eq. (17), in view of Eq. (12), may be written as  $\delta \boldsymbol{\varepsilon}^r = \boldsymbol{\Psi} \boldsymbol{\Delta} \delta \mathbf{d}$ , where

$$\boldsymbol{\Psi} = \begin{bmatrix} \mathbf{Q}^T & \mathbf{Q}^T \mathbf{Z}' \boldsymbol{\Gamma} & \mathbf{O} & \mathbf{o} & \mathbf{o} \\ \mathbf{O} & \mathbf{Q}^T \boldsymbol{\Gamma}' & \mathbf{Q}^T \boldsymbol{\Gamma} & \mathbf{o} & \mathbf{o} \\ \mathbf{o}^T & \mathbf{o}^T & \mathbf{o}^T & 1 & 0 \\ \mathbf{o}^T & \mathbf{o}^T & \mathbf{o}^T & 0 & 1 \end{bmatrix} \quad \text{and} \quad \boldsymbol{\Delta} = \begin{bmatrix} \mathbf{I} \frac{\partial}{\partial x_3} & \mathbf{O} & \mathbf{O} & \mathbf{o} & \mathbf{o} \\ \mathbf{O} & \mathbf{I} & \mathbf{I} \frac{\partial}{\partial x_3} & \mathbf{o} & \mathbf{o} \\ \mathbf{o}^T & \mathbf{o}^T & \mathbf{o}^T & 1 & \mathbf{I} \frac{\partial}{\partial x_3} \end{bmatrix}^T. \quad (19)$$

The external virtual work of the rod is given by

$$\delta W_{ext} = \int_L \left( \int_C \bar{\mathbf{t}} \cdot \delta \mathbf{x} dC + \int_A \bar{\mathbf{b}} \cdot \delta \mathbf{x} dA \right) dL \quad (20)$$

\* Contribuição tecnocientífica ao **Construmetal 2016** – Congresso Latino-americano da Construção Metálica – 20 a 22 de setembro de 2016, São Paulo, SP, Brasil.

in which  $\bar{\mathbf{t}}$  is the external surface traction acting on the rod's surface per unit reference area,  $C$  is the contour of the cross-sections, and  $\bar{\mathbf{b}}$  is the vector of external body forces per unit reference volume. With  $\delta\mathbf{x}$  above given from linearization of Eq. (2), evaluation of the contour and area integrals in Eq. (20) renders the external force resultants. They are grouped into vector  $\bar{\mathbf{q}}$  as shown below:

$$\bar{\mathbf{q}} = \begin{bmatrix} \bar{\mathbf{n}} \\ \bar{\mathbf{B}} \end{bmatrix}, \quad \text{where} \quad \bar{\mathbf{n}} = \int_C \bar{\mathbf{t}} dC + \int_A \bar{\mathbf{b}} dA$$

$$\bar{\mathbf{m}} = \int_C (\mathbf{a} + \psi p \mathbf{e}_3) \times \bar{\mathbf{t}} dC + \int_A (\mathbf{a} + \psi p \mathbf{e}_3) \times \bar{\mathbf{b}} dA \quad (21)$$

$$\bar{\mathbf{B}} = \int_C \psi \bar{\mathbf{t}} \cdot \mathbf{e}_3 dC + \int_A \psi \bar{\mathbf{b}} \cdot \mathbf{e}_3 dA.$$

allowing us to rewrite Eq. (20) as

$$\delta W_{ext} = \int_L (\bar{\mathbf{q}} \cdot \delta \mathbf{d}) dL. \quad (22)$$

Components of  $\bar{\mathbf{n}}$  and  $\bar{\mathbf{m}}$  are respectively the resultant external forces and moments, whereas  $\bar{\mathbf{B}}$  is the resultant external bi-moment, all per unit reference length of the rod axis.

The equilibrium of the rod is enforced by means of the virtual work theorem in a standard way:

$$\delta W = \delta W_{int} - \delta W_{ext} = 0 \quad \text{in } L, \quad \forall \delta \mathbf{d} \mid \delta \mathbf{d}(0) = \delta \mathbf{d}(l) = \mathbf{o}, \quad (23)$$

with  $\delta W_{int}$  and  $\delta W_{ext}$  given by Eqs. (15) and (20) or by Eqs. (18) and (22). The Fréchet derivative of the above weak form with respect to  $\mathbf{d}$  leads to the tangent formulation of this model:

$$\delta(\delta W) = \int_L ((\mathbf{D}\Psi\Delta\delta\mathbf{d}) \cdot (\Psi\Delta\delta\mathbf{d}) + (\mathbf{G}\Delta\delta\mathbf{d}) \cdot (\Delta\delta\mathbf{d}) - (\mathbf{L}\delta\mathbf{d} \cdot \delta\mathbf{d})) dL, \quad (24)$$

in which

$$\mathbf{D} = \frac{\partial \boldsymbol{\sigma}^r}{\partial \boldsymbol{\varepsilon}^r}, \quad \mathbf{G} = \frac{\partial \Psi^T \boldsymbol{\sigma}^r}{\partial (\Delta \mathbf{d})} \quad \text{and} \quad \mathbf{L} = \frac{\partial \bar{\mathbf{q}}}{\partial \mathbf{d}}. \quad (25)$$

They represent the constitutive effects, the geometric effects of the internal forces and the geometric effects of the external loading on the tangent operator. Operators  $\mathbf{G}$  and  $\mathbf{L}$  are

$$\mathbf{G} = \begin{bmatrix} \mathbf{O} & \mathbf{G}_{u'\theta} & \mathbf{O} & \mathbf{o} & \mathbf{o} \\ \mathbf{G}_{u'\theta}^T & \mathbf{G}_{\theta\theta} & \mathbf{G}_{\theta\theta'} & \mathbf{o} & \mathbf{o} \\ \mathbf{O} & \mathbf{G}_{\theta\theta'}^T & \mathbf{O} & \mathbf{o} & \mathbf{o} \\ \mathbf{o}^T & \mathbf{o}^T & \mathbf{o}^T & 0 & 0 \\ \mathbf{o}^T & \mathbf{o}^T & \mathbf{o}^T & 0 & 0 \end{bmatrix} \quad \text{and} \quad \mathbf{L} = \begin{bmatrix} L_{uu} & L_{u\theta} & L_{up} \\ L_{\theta u} & L_{\theta\theta} & L_{\theta p} \\ L_{pu} & L_{p\theta} & L_{pp} \end{bmatrix} \quad (26)$$

They are given in detail in Pimenta and Yojo (1993) and Campello (2000). Observe that if  $\mathbf{D}$  is symmetric and the external loading is conservative, the tangent operator will also be symmetric. Expressions for  $\mathbf{D}$  will be developed in the following chapter.

### 3. ELASTOPLASTIC CONSTITUTIVE EQUATION

#### 3.1. Model for small strains and large displacements and rotations

For the elastic regimen of deformation, we assume that the behavior of the material is governed by the classic Kirchhoff-Saint Venant model, which states that

$$\mathbf{S} = \lambda(\mathbf{I} : \mathbf{E} + 2\mu\mathbf{E}) \quad (27)$$

\* Contribuição tecnocientífica ao **Construmetal 2016** – Congresso Latino-americano da Construção Metálica – 20 a 22 de setembro de 2016, São Paulo, SP, Brasil.

in which  $\lambda$  and  $\mu$  are the Lamé parameters,  $\mathbf{E}$  is the Green-Lagrange strain tensor and  $\mathbf{S}$  is the second Piola-Kirchhoff stress tensor. For homogeneous isotropic materials, the Lamé parameters can be written in terms of the elastic modulus  $E$  and shear modulus  $G$  as (Gaussmann, 1951):

$$\mu = G \quad \text{and} \quad \lambda = \frac{G(E - 2G)}{3G - E}. \quad (28)$$

In this case, it can be shown that, up to the first order,  $\mathbf{Q}^T \mathbf{P} = \mathbf{P}^r \approx \mathbf{S}$  (Campello, 2000, p. 49) and Eq. (15) of the internal virtual work can be rewritten as

$$\delta W_{int} = \int_L \int_A (\mathbf{S} : \delta \mathbf{E}) dA dL \quad (29)$$

This relation allows us a simple expression for the back-rotated stress vector  $\tau_{33}^r$ . We start with the Green-Lagrange strain tensor  $\mathbf{E}$ , energetically conjugated to  $\mathbf{S}$ , that is

$$\mathbf{E} = \frac{1}{2}(\mathbf{F}^{rT} \mathbf{F}^r - \mathbf{I}) = \frac{1}{2} \left( \begin{bmatrix} 1 & 0 & p\psi_{,1} \\ 0 & 1 & p\psi_{,2} \\ \gamma_{31}^r & \gamma_{32}^r & \gamma_{33}^r \end{bmatrix} \begin{bmatrix} 1 & 0 & \gamma_{31}^r \\ 0 & 1 & \gamma_{32}^r \\ p\psi_{,1} & p\psi_{,2} & \gamma_{33}^r \end{bmatrix} - \mathbf{I} \right) \quad (30)$$

where  $\gamma_{3\alpha}^r$  and  $\gamma_{33}^r$  are the components of  $\gamma_3^r$ . Keeping only the first order terms in these component products yields

$$\mathbf{E} = \frac{1}{2} \begin{bmatrix} 0 & 0 & \gamma_{31}^r + p\psi_{,1} \\ 0 & 0 & \gamma_{32}^r + p\psi_{,2} \\ \gamma_{31}^r + p\psi_{,1} & \gamma_{32}^r + p\psi_{,2} & 2\gamma_{33}^r \end{bmatrix}. \quad (31)$$

Replacing Eq. (31) and Eq. (28) in Eq. (27), we obtain the classic linear elastic relations for all stresses in  $\mathbf{P}^r \approx \mathbf{S}$  which, in components, reads as

$$\mathbf{S} = \begin{bmatrix} \lambda \gamma_{33}^r & 0 & \mu(\gamma_{31}^r + p\psi_{,1}) \\ 0 & \lambda \gamma_{33}^r & \mu(\gamma_{32}^r + p\psi_{,2}) \\ \mu(\gamma_{31}^r + p\psi_{,1}) & \mu(\gamma_{32}^r + p\psi_{,2}) & (\lambda + 2\mu)\gamma_{33}^r \end{bmatrix}.$$

Converting the material parameters we get

$$\mathbf{S} = \begin{bmatrix} \left(\frac{G(E-2G)}{3G-E}\right) \gamma_{33}^r & 0 & G(\gamma_{31}^r + p\psi_{,1}) \\ 0 & \left(\frac{G(E-2G)}{3G-E}\right) \gamma_{33}^r & G(\gamma_{32}^r + p\psi_{,2}) \\ G(\gamma_{31}^r + p\psi_{,1}) & G(\gamma_{32}^r + p\psi_{,2}) & \left(2G + \frac{G(E-2G)}{3G-E}\right) \gamma_{33}^r \end{bmatrix}.$$

Observing the components of  $\mathbf{E}$  in Eq. (31) that are zero, the components of  $\mathbf{S}$  that will contribute to the internal virtual work are:

$$\tau_{3\alpha}^r = \tau_{\alpha 3}^r = G(\gamma_{3\alpha}^r + p\psi_{,\alpha}) \quad \text{and} \quad \tau_{33}^r = \frac{G(4G - E)}{3G - E} \gamma_{33}^r \quad (32)$$

where  $\tau_{33}^r$  and  $\tau_{3\alpha}^r$  are the components of  $\tau_3^r$  and correspond to the cross-sectional normal and shear stresses respectively. Observe that for materials with  $E \approx 2G$  we have  $\tau_{33}^r = E\gamma_{33}^r$  and that a relation of  $E = 3G$  implies that Poisson's ratio  $\nu = 0.5$  and the material would be perfectly incompressible.

With these relations in Eq. (16) we can obtain the tangent matrix  $D = \partial\sigma/\partial\varepsilon$  of constitutive effects.

When in plastic deformation regimen, we assume that the material behavior of the rod is described by the classical elastoplastic constitutive model for small strains. Accordingly, using superscripts  $|e$  and  $|p$  for elastic and plastic parts respectively, the cross-sectional strain vector  $\gamma_3^r$  of Eq. (6) is decomposed additively as

$$\gamma_3^r = \gamma_3^{r|e} + \gamma_3^{r|p}. \quad (33)$$

Furthermore, the plastic strain  $\gamma_3^{r|p}$  is assumed to occur due only to the cross-sectional normal stress  $\tau_{33}^r$  from Eq. (14). This allows us to work under a simple uniaxial framework for the plastic deformations. With these deformation components and considering the linear elastic relation of the Kirchhoff-St. Venant material, we formulate the elastic stress-strain relationship governing  $\tau_{33}^r$  and  $\gamma_{33}^{r|e}$  as

$$\tau_{3\alpha}^r = \tau_{\alpha 3}^r = G(\gamma_{3\alpha}^r + p\psi_{,\alpha}) \quad (34)$$

$$\tau_{33}^r = \frac{G(4G - E)}{3G - E} \gamma_{33}^{r|e} = \frac{G(4G - E)}{3G - E} (\gamma_{33}^r - \gamma_{33}^{r|p}). \quad (35)$$

Considering isotropic hardening of the material that follows Ludwik's hardening law, the admissible stresses for this component lie within the following conditions:

$$\mathcal{F}(\tau_{33}^r, \alpha) = |\tau_{33}^r| - (\sigma_Y + K\alpha^m) \leq 0 \quad \text{and} \quad \alpha \geq 0 \quad (36)$$

where  $\mathcal{F}$  is the yield criterion,  $\sigma_Y$  is the initial yield stress,  $\alpha$  is the internal hardening variable,  $K$  is the strength coefficient and  $m$  is the strain hardening exponent. We adopt an associative plastic flow rule and a simple evolutionary equation for the hardening variable as equivalent plastic strain given by

$$\dot{\gamma}_{33}^{r|p} = \dot{\alpha}\hat{n} \quad \text{and} \quad \dot{\alpha} = |\dot{\gamma}_{33}^{r|p}| \quad \text{where} \quad \hat{n} = \frac{\partial\mathcal{F}}{\partial\tau_{33}^r} \quad (37)$$

The Kuhn-Tucker loading/unloading conditions and the consistency condition are then expressed as

$$\mathcal{F} \leq 0, \quad \dot{\alpha} \geq 0, \quad \dot{\alpha}\mathcal{F} = 0 \quad \text{and} \quad \dot{\alpha}\dot{\mathcal{F}} = 0 \quad (38)$$

With these conditions it is possible to characterize the material behavior in the elastic and plastic states when subject to loading or unloading:

$$\begin{array}{l} \text{elastic :} \\ \text{plastic :} \end{array} \left\{ \begin{array}{lll} \text{loading :} & \mathcal{F} < 0, & \dot{\mathcal{F}} > 0, & \dot{\alpha} = 0 \\ \text{unloading :} & \mathcal{F} < 0, & \dot{\mathcal{F}} < 0, & \dot{\alpha} = 0 \\ \text{loading :} & \mathcal{F} = 0, & \dot{\mathcal{F}} = 0, & \dot{\alpha} > 0 \\ \text{unloading :} & \mathcal{F} = 0, & \dot{\mathcal{F}} < 0, & \dot{\alpha} = 0 \end{array} \right.$$

To implement this constitutive model within the kinematics described in the previous section, we recover the internal virtual work from Eqs. (11), (12) and (15) and write it in terms of  $\tau_i^r$  and  $\delta\gamma_3^r$ :

$$\begin{aligned} \delta W_{int} &= \int_L \int_A (\mathbf{P} : \delta\mathbf{F}) dA dL \\ &= \int_L \int_A \tau_{\alpha 3}^r \delta\gamma_{\alpha 3}^r + \boldsymbol{\tau}_3^r \cdot (\delta\boldsymbol{\eta}^r + \delta\boldsymbol{\kappa}^r \times (\mathbf{a}^r + \psi p \mathbf{e}_3^r) + \psi \delta p' \mathbf{e}_3^r + \psi \delta p \boldsymbol{\kappa}^r \times \mathbf{e}_3^r) dA dL \\ &= \int_L \int_A \tau_{\alpha 3}^r \delta\gamma_{\alpha 3}^r + \boldsymbol{\tau}_3^r \cdot \delta\boldsymbol{\gamma}_3^r dA dL \end{aligned} \quad (39)$$

\* Contribuição tecnocientífica ao **Construmetal 2016** – Congresso Latino-americano da Construção Metálica – 20 a 22 de setembro de 2016, São Paulo, SP, Brasil.



### 3.2. Stress integration algorithm

To implement the stress integration algorithm, specifically the well-known return mapping algorithm for the uni-dimensional case (Simo and Hughes, 1998), we replace the stress, strain and hardening rates by finite increments. It allows us to perform the analysis using an incremental loading scheme.

At the start of the analysis, variables for the hardening and plastic strains are initialized and have their history stored to be used in later steps. We compute the elastic trial stress  $\tau_{33n+1}^{r \text{ trial}}$  as part of the same finite element models of Campello and Lago (2014) and described in section 2 and Eq. (39). From this stress component we compute  $\mathcal{F}$  and verify the compliance with the yield criterion. Here, the hardening variable from the previous step must be provided:

$$\tau_{33n+1}^{r \text{ trial}} = \frac{G(4G - E)}{3G - E} (\gamma_{33n+1}^r - \gamma_{33n}^{r|p}) \quad (40)$$

$$\mathcal{F}_{n+1}^{\text{trial}} = |\tau_{33n+1}^{r \text{ trial}}| - (\sigma_Y + K\alpha_n^m) \quad (41)$$

If  $\mathcal{F}_{n+1}^{\text{trial}} \leq 0$ , the model is either in elastic state or in neutral loading, and the stress and strain are effectively the trials computed. The hardening variables do not change in this case. However, if the yield criterion is not fulfilled, the trial stress is projected to the yield surface and the plastic strain and hardening variables are incremented:

$$\Delta\alpha = \frac{\mathcal{F}_{n+1}^{\text{trial}}}{\frac{G(4G-E)}{3G-E} + Km\alpha_{n+1}^{m-1}} \quad \text{if } \mathcal{F}_{n+1}^{\text{trial}} > 0, \quad \text{else } \Delta\alpha = 0, \quad (42)$$

$$\alpha_{n+1} = \alpha_n + \Delta\alpha \quad (43)$$

$$\gamma_{33n+1}^{r|p} = \gamma_{33n}^{r|p} + \hat{n}\Delta\alpha \quad \text{with } \hat{n} = \frac{\tau_{33n+1}^{r \text{ trial}}}{|\tau_{33n+1}^{r \text{ trial}}|}, \quad (44)$$

$$\tau_{33n+1}^r = \frac{G(4G - E)}{3G - E} (\gamma_{33n+1}^r - \gamma_{33n+1}^{r|p}). \quad (45)$$

To solve the nonlinear Eq. (42) when  $\mathcal{F}_{n+1}^{\text{trial}} > 0$ , we use a local iterative Newton procedure. Since there is no kinematic hardening, the target function simplifies to the yield criterion  $\mathcal{F}$  which is convex, so the convergence of the Newton procedure is guaranteed. Iterating in  $k$  steps, it is as follows:

$$\text{initialize } \Delta\alpha_0 = 0, \quad \alpha_0 = \alpha_n \quad (46)$$

$$\text{if } \mathcal{F}_{n+1}^{\text{trial}}(\alpha_k) \leq 0, \quad \Delta\alpha = \Delta\alpha_k \quad (47)$$

$$\text{else } \Delta\alpha_{k+1} = \frac{\mathcal{F}_{n+1}^{\text{trial}}(\alpha_k)}{\frac{G(4G-E)}{3G-E} + Km\alpha_k^{m-1}} \quad (48)$$

$$\alpha_{k+1} = \alpha_n + \Delta\alpha_{k+1} \quad (49)$$

$$k \leftarrow k + 1.$$

### 3.3. Integration over the cross-section

To compute the stress resultants of Eq. (16), the integration over the cross-section is needed and it cannot be performed analitically because of the progressive plastification of the cross-section. For this implementation, the procedures described above are broken down into a series of steps

\* Contribuição tecnocientífica ao **Construmetal 2016** – Congresso Latino-americano da Construção Metálica – 20 a 22 de setembro de 2016, São Paulo, SP, Brasil.

to account for this integration and also to provide an adequate model for partial plastification of the cross-sections of the rod. As seen in Eq. (6), the dependence of  $\gamma_3^r$  on coordinates over the cross-section is gathered in the vector  $\mathbf{a}^r = x_\alpha \mathbf{e}_\alpha$ . For this elastoplastic constitutive model, we use an integration scheme similar to that in Campello and Lago (2014). The integration over the cross-section is approximated numerically using a 2-dimensional mesh. For every cell of this cross-sectional mesh we compute the quantities that depend on  $\mathbf{a}^r$  using the coordinates of the midpoint and weight this contribution with the area  $s$  of the cell.

$$\int_A (\bullet) dA \simeq \sum_A (\bullet)_s \quad (50)$$

The stress integration algorithm above is then applied to components  $\tau_{33}^r$  and  $\gamma_{33}^r$  of the stress and strain vectors and to the internal hardening  $\alpha$  and plastic strain  $\gamma_{33}^{r|p}$  for each of these cells. After that, the tangent matrix and residuum vector can be assembled as in the elastic model.

The warping function used in this implementation is obtained exactly by employing the finite element method using the cross-sectional mesh to solve the following variational problem

$$\int_A \nabla v \cdot \nabla \psi dA - \int_A \nabla v \cdot \mathbf{g} dA = 0 \quad \text{where} \quad \mathbf{g} = \begin{bmatrix} 0 & 1 \\ -1 & 0 \end{bmatrix} \mathbf{a}^r, \quad (51)$$

$v$  is a test function and  $\psi$  is the warping function. We assume that  $\psi$  remains unchanged in the plastic deformation regimen.

#### 4. NUMERICAL EXAMPLES

The formulation presented in the previous Section was implemented in the finite element models of the works of Pimenta and Yojo (1993), Campello (2000), Campello and Pimenta (2001) and Campello and Lago (2014). Both 2-node and 3-node rod elements (linear and quadratic interpolation functions for all degrees-of-freedom of Eq. (4)) were considered. To resolve the constitutive equation, computation of the stress resultants of Eq. (16) was performed via integration over the cross-section as mentioned. Reduced Gaussian quadrature was used for integration over the rod's length. A Newton incremental/iterative solution scheme is adopted.

We performed several numerical tests in order to validate the implementation. We analyzed examples involving compression, bending, torsion and warping. The results obtained were excellent and compared very well with reference solutions whenever these were available (both in nodal solution and in stress resultants). For the sake of simplicity, we show here the results of only a few of these tests.

For all examples, a triangle mesh is used for the cross-section. The results over the cross-section correspond, on the axis, to the nearest quadrature point in cases of results on the middle or the end of the rod. To improve the approximation of these results, the axis mesh is refined around the critical cross-section. These results are for the formulation without warping of the cross-section. Results with warping cross-sections and reference solutions are being prepared and will be ready in the near future.

#### ACKNOWLEDGEMENTS

First author acknowledges CAPES (Brazilian Agency of Graduate Education from Ministry of Education) for the research grant given through the Postgraduate Program in Civil Engineering of the Polytechnic School of the University of São Paulo.

Second author acknowledges CNPq (Conselho Nacional de Desenvolvimento Científico e Tecnológico) for the research grant 303793/2012-0.

\* Contribuição tecnocientífica ao **Construmetal 2016** – Congresso Latino-americano da Construção Metálica – 20 a 22 de setembro de 2016, São Paulo, SP, Brasil.

## REFERENCES

- CAMPELLO, E. M. B. (2000) *Nonlinear Analysis of cold-formed steel members*. Dissertation (Master) (in Portuguese). Department of Structural and Geotechnical Engineering, University of São Paulo.
- CAMPELLO, E. M. B., LAGO, L. B. (2014) *Effect of higher order constitutive terms on the elastic buckling of thin-walled rods*. *Thin Walled Structures* 77:8-16.
- CAMPELLO, E. M. B., PIMENTA, P. M. (2001) *Geometrically nonlinear analysis of thin-walled space frames*. In: Proceedings of the Second European Conference on Computational Mechanics (II ECCM). Cracow.
- GAUSSMANN, F. (1951) *Über die elastizität poroser medien. (On elasticity of porous media)*. *Vierteljahrsschrift der Naturforschenden Gessellschaft in Zurich*, 96, p. 1-23.
- PIMENTA, P. M., YOJO, T. (1993) *Geometrically exact analysis of spatial frames with consideration of torsion warping*. In: Proceedings of the XVI Iberian-Latin-American Congress on Computational Methods in Engineering (XVI CILAMCE), São Paulo, p. 21-30.
- SIMO, J. C.; HUGHES, T. J. R. (1998) *Computational Inelasticity*. New York: Springer. (Interdisciplinary Applied Mathematics, v. 7).
- SIMO, J. C., VU-QUOC, L. (1986) *A three-dimensional finite strain rod model. Part II: Computational Aspects*. *Comput Methods Appl Mech Eng* 58:79-116.
- SIMO, J. C., VU-QUOC, L. (1991) *A geometrically exact rod model incorporating shear and torsion-warping deformation*. *International Journal of Solids and Structures* 27:371-93.
- VLASOV, V. Z. (1961) *Thin-walled elastic beams*. Jerusalem, Israel. Program for Scientific Translation.